Compact High Gain Multiband Antenna Based on Split Ring Resonator and Inverted F Slots for 5G Industry Applications

Ranjan Mishra [1], Rajeev Dandotiya [1], Ankush Kapoor [2], and Pradeep Kumar [3]

[1] Department of Electrical and Electronics Engineering, University of Petroleum and Energy Studies, Dehradun, India
rmishra@ddn.upes.ac.in, rajeevdandotiya@gmail.com

[2] Department of Electronics and Communication Engineering, Jawaharlal Nehru Government Engineering College
Sundernagar, Mandi, India
ankush8818@yahoo.com

[3] Discipline of Electrical, Electronic and Computer Engineering, University of KwaZulu-Natal
Durban-4041, South Africa
pkumar_123@yahoo.com

Abstract ─ This paper presents the design, optimization, fabrication, and measurement of the compact high gain microstrip antenna with a split ring resonator and set of inverted-F slots along with a matching stub for sub-6 GHz5G applications. In this investigation, different iterations are visualized by incorporating inverted F slots, a split ring resonator, and a matching stub in the transmission line. The advantages of each incorporated structure are analyzed, and a hybrid antenna consisting of the combination is proposed as a final antenna configuration with the optimum results. The proposed final design attains compactness and multi-band operation. Impedance matching is improved by using the stub matched technique at the feed line. The designed antenna shows the resonances at precisely 2.1 GHz, 3.3 GHz, and 4.1GHz. The proposed antenna is suitable for mobile cellular communication such as the LTE band (2.1 GHz), n78 band (3.3 GHz), and n77 band (4.1 GHz) of 5G bands. The gain retrieved from each band attains more than 5 dB value.

Index Terms ─ Fifth generation (5G), inverted F-slot, Split Ring Resonator (SRR), stub matching.

I. INTRODUCTION

In the 21st century, wireless communication and networking devices require multiple operating frequencies due to the rapid increase in the demand of users. This demand for multi-band operated antennas needs to cater to compactness in dimensions while maintaining the performance characteristics. These reasons are sufficient for going to the design of a multi-band antenna. Multiband antennas are becoming an eye of sight for researchers in applications with a need for downward compatibility and adequate facilities. With the rise of LTE and demand for 5G technology, there is always a need for multi-band antennas. High data rate and increasing users for data transmission systems have motivated researchers to develop multi-band antennas. In recent years, researchers have made various efforts to get the multi-band operation by using patch antennas. A patch antenna with a T-shaped slit on the radiating aperture has shown a multi-band operation with operating frequencies at 3.92 GHz and 5.82 GHz of C band, and 7.88 GHz and 11.35 GHz of X band of microwave spectrum [1]. A planar MIMO antenna structure integrated with mm-wave has been discussed [2] for future V2X applications. This phased array antenna structure is used in LTE/sub-6 GHz 5G and the miniaturization was achieved using a gap capacitor and inter digital capacitors. Further, a multi-band antenna array structure suitable for smart phones operating in LTE bands 42/43/46 has been presented using two diverse open slots on a T-shaped slot antenna [3]. Sub-6 GHz has taken the interest of researchers in designing the antenna, radio frequency circuits, and spatial filters [4]. A simple single feed design is proposed for a multi-band antenna with defected ground substrate structure [5]. A compact slot antenna with the 3 L-shaped slots and the ground plane for three operating frequency bands is proposed in [6]. A compact F-shaped slot antenna showing multi-band frequency is proposed, and its application area is focused on WLAN, Wi-MAX, and X band applications [7]. In [8], the design of a four-band antenna is presented, and the structure involves a T-shaped feed patch, an inverted T-shaped stub, and two E-shaped stubs. Further investigations have been done in designing a partial slotted ground antenna for wideband applications [9]. Further in [10], patch antennas for sub-6 GHz 5 G communications have a T slot on a

Submitted On: March 23, 2021
Accepted On: July 7, 2021
https://doi.org/10.47037/2021.ACES.J.360808

rectangular patch and a defective ground structure. A wideband antenna, with gain enhancement using FSS based spatial filters, is presented for operation in less than 6 GHz of frequency [11]. A compact reconfigurable 3-D slot antenna suitable for 5G mobile application is offered with a metal casing [12]. In [13], a dual multi-band planar inverted F antenna system is proposed in which the bandwidth is enhanced by using a specific configuration of slots. A design of an inverted F slot antenna structure has claimed to be easily integrated into handheld devices or printed on WLAN card is proposed [14]. In [15], a new planar inverted-F antenna with a very large bandwidth starting from 817 MHz to 11.5 GHz is proposed as an alternative for high performance mobile phones and also intended to cover the major part of the mobile phone frequencies as well as the ultra-wideband (UWB) frequency range. The research on multi-band antennas has been extended in which a dual-band antenna consisting of a rectangular patch fed by the coaxial probe feeding technique and a ground plane loaded with two rectangular strip slots and one elliptical slot is proposed [16]. Further, a compact triple-band microstrip antenna, with a rectangular stub connected to the feed line, is proposed for tri-band applications [17]. The proposed antenna covers 2.1-2.8 GHz, 3.3-4.0 GHz, and 5.5-5.8 GHz. A triple-band microstrip antenna consisting of a slotted rectangular patch with the defected ground is designed for triple-band operation at 1.2 GHz, 2.45 GHz, and 5.6372 GHz [18]. In [19], the PIFA is proposed employing a rectangular split-ring resonator structure exhibiting multi-band characteristics and suitable for mobile applications.

In this paper, a design of multi-band antenna is recommended by incorporating fractal slots, inverted F-slots, and split ring resonator. The antenna shows multi-band behavior with an adequate value of gain and finds its applications in sub-6 GHz applications.

The manuscript is organized as follows. The antenna geometry is described in Section II. Section III is devoted to measuring and validating the results, and finally, the conclusion is briefed in Section IV.

II. ANTENNA GEOMETRY

This section presents the design and the optimization of an inverted-F slot microstrip antenna for sub-6 GHz band in 5G application. In this investigation, an inverted-F slot on the antenna patch is designed to get the multi-band operations with a higher order of miniaturization. Impedance matching is improved by using a stub matched technique at the feed line. The designed antenna shows a perfect resonance at 2.1 GHz, 3.3 GHz, and 4.1 GHz of the frequency with a good reflection coefficient. The gain of each band is more than 5dB. These three frequencies are chosen for LTE (2.1 GHz), n77 band of 5G (3.3 GHz), and n78 band of 5G (4.1 GHz), respectively, as per ITU-NR and department of telecommunications (DOT), Government of India proposal for 5G applications [20]-[21]. The proposed antenna geometry considers a square fractal aperture with microstrip line feeding. The feeding is optimized with stub matching to improve the reflection coefficient characteristics and provide operability in the 5G applications. The square aperture of the antenna is first optimized by the combination of inverted-F slots at the diagonal corner to improve the performance of the antenna. A split ring slot is dogged just after the feed line, which cooperatively improves the radiation characteristics of the designed antenna. The proposed antenna demonstrates three resonance bands, the first one is at 2.1 GHz, and the second one is at 3.3 GHz, while the third one is at 4.1 GHz of frequency. Typically gain at each resonance is enhanced to more than 4 dB and with a good radiation pattern. The combined fractal and slotted configuration realize multi-band operation applicable for the mobile communication system. The proposed antenna is suitable for mobile cellular communications such as LTE band (2.1 GHz) and 5G-NR (3.3 GHz and 4.1 GHz) communication bands. A compact microstrip inverted-F slotted fractal antenna for mobile and 5G-NR applications is presented. In this investigation, the inverted-F slot on the antenna aperture is analyzed to demonstrate multi-band mobile operations with a higher order of miniaturization. The impedance matching is improved by using a stub-matched technique with offset feeding. The substrate chosen for this design is RT-duroid (RT 5880) substrate, having a dielectric constant value of 2.2, and a loss tangent of 0.009. Substrates of low tangent losses will minimize dielectric losses, but these substrates are costly. The chosen height of the substrate is 1.57 mm and using this moderate thicker substrate, conductor losses may also be minimized, thereby influencing the antenna's performance. This RT-duroid substrate is although expensive, but at the same time, enhances the performance in terms of reflection coefficient and gain. The aim in choosing this specification is to design a multi-band antenna with good gain, reflection coefficient, and directive radiation property. The design is proposed to find its scope in the modern wireless mobile communication system. Primarily the physical dimensions are determined using the equations given below [22].

The width of the patch, W_p, is given as:

$$W_P = \frac{c}{2f}\sqrt{\frac{2}{(\varepsilon_r+1)}}, \quad (1)$$

where c, f and $\boldsymbol{\varepsilon}_r$ denote the velocity of light, the resonant frequency andthe relative permittivity, respectively.

The length of the patch, L_p, is given as:

$$L_P = L_{eff} - 2\Delta L, \quad (2)$$

where ΔL denotes the extended effective length. The effective length, L_{eff}, is given as below:

$$L_{eff} = \frac{c}{2f\sqrt{\varepsilon_{eff}}}. \quad (3)$$

The effective dielectric constant, ε_{eff}, of the substrate, is given as:

$$\varepsilon_{eff} = \frac{\varepsilon_r+1}{2}+\frac{\varepsilon_r-1}{2}\sqrt{\left[1+\frac{12h}{W_p}\right]}, \quad (4)$$

where h denotes the thickness of the substrate. By considering the normalized extension, the actual length of patch, L_p, is given as:

$$L_P = \frac{c}{2f}\left(\frac{\varepsilon_r+1}{2}+\frac{\varepsilon_r-1}{2}\sqrt{\left[1+\frac{12h}{W}\right]}\right)^{-\frac{1}{2}} - 2\Delta L. \quad (5)$$

The design flow of the proposed antenna has gone through little iteration. A conventional rectangular patch is implemented on the top surface of dielectric substrate wherein a fully conductive ground is considered. In the first iteration, fractal slots are engraved at the opposite boundaries along the length of the patch for making the design a fractal slot based rectangular patch antenna (FSRPA). Fractal slot is derived from the self-identical and broken irregular pieces, belonging to a family of intrinsic geometrical structures [23]. The geometrical layout along with the dimensional parameters is illustrated in Fig. 1 (a). A fractal slot carved on the edge along the length of the antenna produces different frequency bands owing to its repeating geometry structure. The microstrip patch antenna embedded with the modified fractal design exhibited a dual frequency response. This antenna provides resonance at various frequencies in the band due to its fractal design. In the next step of the design iteration, a dual inverted plane F slot is introduced on the radiating patch (DIFRPA). The DIFRPA consists of F-slots structures that lie opposite to each other as demonstrated in Fig. 1 (b). However, the design of Fig. 1 (a) produces the multi resonance characteristic, but the performance is not good in terms of reflection coefficient for the specified bands. This shortcoming leads to the second design. The second design of Fig. 1 (b) also illustrates the three well distinguishable bands, but the second band doesn't give a good reflection coefficient. Moreover, the three bands are still not falling precisely as per the specified frequency. The objective of exact resonance at a specific frequency enables the structure of the third design. The third design of Fig. 1 (c) consists of stub matching (SMRPA) helps to achieve triple-band operation with the narrow bandwidth. The improvement is required in the third design for better matching impedance between the source and the antenna. This inverted F structure is also used in controlling the frequency and to enhance the gain by improving impedance matching and reducing the backward radiation [24]-[26].

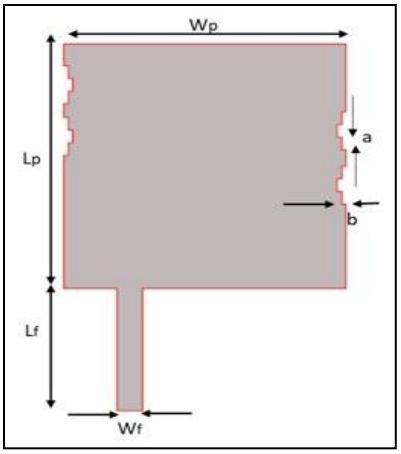

(a)

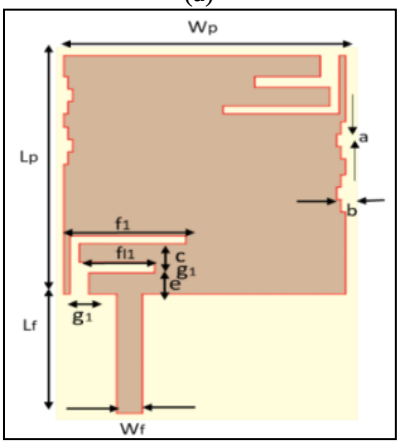

(b)

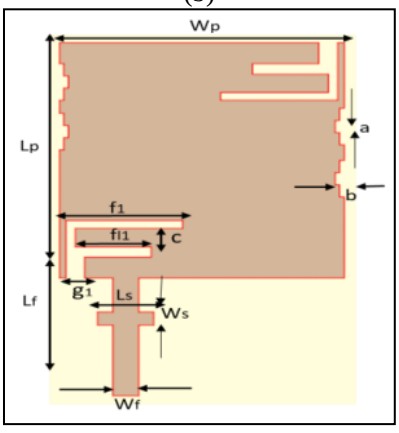

(c)

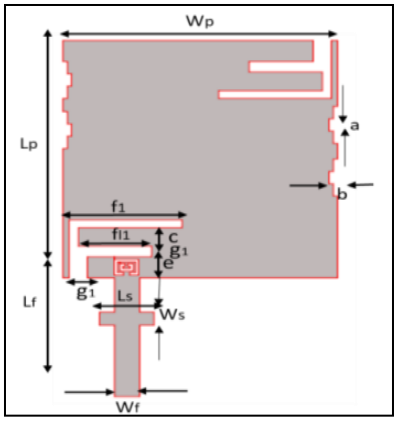

(d)

Fig. 1. Design evolution steps of the proposed antenna, (a) FSRPA, (b) DIFRPA, (c) SMRPA, and (d) SRRRPA.

In short, this structure consists of radiating patches parallel to a ground that is joined to the ground by a shorting plate to resonate at a quarter wavelength. The impact of the inverted-F slot over the fractal slot-loaded square patch antenna is to bring the first resonance at 2.2 GHz and the second resonance at 3.0 GHz. The designed antenna also demonstrates the third band around 4.2 GHz of frequency and thus results in multiple resonances in sub-6 GHz band, as shown in the reflection coefficient plot depicts in Fig. 2. This design brings the first band at 2.2 GHz. The second band also comes to be at 3.3 GHz, but its resonance is not good, and the radiation is near to -10 dB. The third band is exciting at 4.2 GHz with a poor reflection coefficient. Implementation of multiple slots improves the multi-band response, but it degrades the impedance characteristics. Stub matching technique has been investigated to improve the impedance response at multiple resonances. Analysis has been carried out using different stub size and position. It has been observed that the change in stub dimension gives considerable order flexibility in impedance tuning without disturbing the original resonances. It is realized the stub length (Ls) of 8.9 mm and width (Ws) of 2.5 mm meet the appropriate reflection coefficient response. The comparison of the reflection coefficients obtained from all four designs is shown in Fig. 2. This design brings the first band at 2.2 GHz. The second band also comes to be at 3.0 GHz, but its resonance is not good and the radiation is near to -10 dB. The third band is exciting at 4.2 GHz with a reflection coefficient near -10 dB. The introductions of stub matching improve the three bands' overall reflection coefficient and precisely position the three bands at the desired and specified frequency.

In the last step, a tiny split ring slot is implemented on the patch of the antenna aperture making 4th iteration as split ring resonator based rectangular patch antenna (SRRRPA). This is done to improve the impedance matching of the antenna further to get it excited at the specified frequencies. The position of this slot is just at the junction point of feed line and radiating patch. The final proposed antenna design**,** i.e.**,** SRRRPA is loaded with fractal slots, inverted F slot and split ring, and a stub matching technique to achieve a fine tuning in the impedance profile. All these structures are plane in nature with easily etched on the patch, and the structure of the final designed antenna is shown in Fig. 1 (d). As per Fig. 2, the reflection coefficient curve of the SRRRPA demonstrates that all the three bands are well distinguished, and they are resonating strictly at 2.1 GHz, 3.3 GHz, and 4.1 GHz of the frequency with a reflection coefficient of -28 dB, -21 dB, and -24 dB respectively. The dimensional parameters for the proposed SRRRPA are enumerated in Table 1.

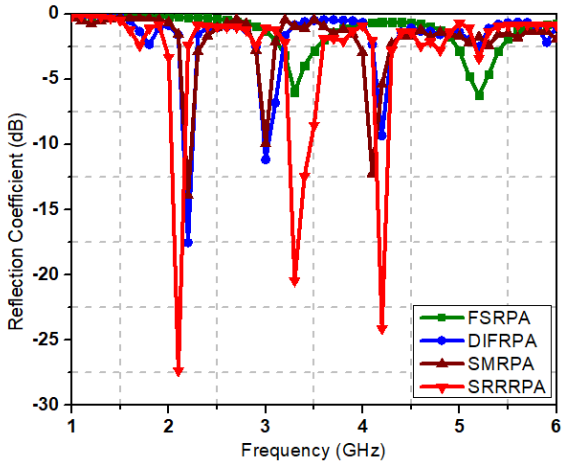

Fig 2. Reflection coefficient of various antenna configurations.

Table 1: Dimensional parameters of the SRRRPA

Parameter	Value
Substrate height (hs)	0.01 λ_{mid}
Patch length, Lp	0.46 λ_{mid}
Patch width, Wp	0.46 λ_{mid}
Feed length (Lf)	0.23 λ_{mid}
Feed width (Wf)	0.04 λ_{mid}
Upper arm of F slot, fl	0.19 λ_{mid}
Lower arm of F slot, fl1	0.12 λ_{mid}
Fractal slot, a	0.02 λ_{mid}
Fractal slot, b	0.007 λ_{mid}
Gap between F slot, c	0.03 λ_{mid}
Distance of f slot, e	0.04 λ_{mid}
Width of base of F slot, g1	0.03 λ_{mid}
Width of arm of F slot, g2	0.02 λ_{mid}
Length of stub, Ls	0.09 λ_{mid}
Width of stub, Ws	0.02 λ_{mid}

Where λ_{mid} is the middle wavelength corresponding to 3.1 GHz. The comparative analysis of the variation of the peak gain along the operating frequency bands is illustrated in Fig. 3. Figure 3 depicts that the antenna has a good gain response of more than 5 dB in the entire zone of its operating frequency for the final design of SRRRPA. The values of the peak gain of SRRRPA at the three bands are 5.4 dB at 2.1 GHz, 6.4 dB at 3.3 GHz, and 5.1 dB at 4.1 GHz.

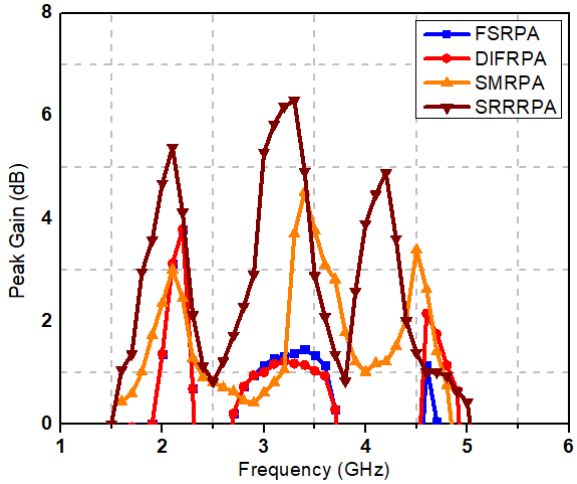

Fig. 3. Peak gain of various antenna configurations.

III. MEASUREMENT VALIDATION

The final antenna design of SRRRPA is fabricated using RT-duroid (Rogers 5880) as dielectric substrate with a height of 1.57 mm. In the fabrication process, a photographic film of the antenna is carved out initially, and then it is glued to the substrate. The patch and the ground of the substrate are copper cladding. In the next stage, the antenna is etched out with a chemical solution. Finally, the fabrication of the antenna is done by a computerized mechanical etching process. In this process, necessary care was taken to align the ground slit exactly below the stub-matched transmission line. Figure 4 shows the photograph of the fabricated antenna.

The reflection coefficient of the fabricated antenna is measured using a vector network analyzer and is validated by comparing it with the simulated results. The gain and the radiation pattern are measured in an anechoic chamber. The measured values of the reflection coefficient with frequency and the simulated results are shown in Fig. 5. The reflection coefficient of the fabricated antenna is measured using a vector network analyzer and validated by comparing it with the simulated results. The gain and the radiation are measured in an anechoic chamber. As demonstrated, the experimental analysis follows the resonance characteristics precisely the same as that of the simulation work with a very nominal deviation. The experiment analysis validates the claimed resonances at 2.1 GHz, 3.3 GHz, and 4.1 GHz of the frequency with reflection coefficient -19 dB, -17 dB, and -18 dB, respectively. The plot for gain response is shown in Fig. 6, and it depicts that the measured peak gain at three bands is 4.6 dB, 5.5 dB, and 4.1 dB, respectively. The E-plane and H-plane plot for all the resonance frequencies (both measured and simulated) are shown in Fig. 7, respectively. The radiation pattern of the E-plane demonstrates that the measured results are in accordance with the simulated design work. The maximum radiation intensity is towards the principal lobe of the antenna, and the back lobe is almost null. It depicts the directive nature of the radiation. The measurement of H-plane results reveals that the radiation intensity is concentrated more towards the main lobe. The main lobe is dominating with almost no presence of back lobe radiation. The radiation pattern also clearly shows the directive nature of the radiation.

Fig. 4. Prototype of the SRRRPA.

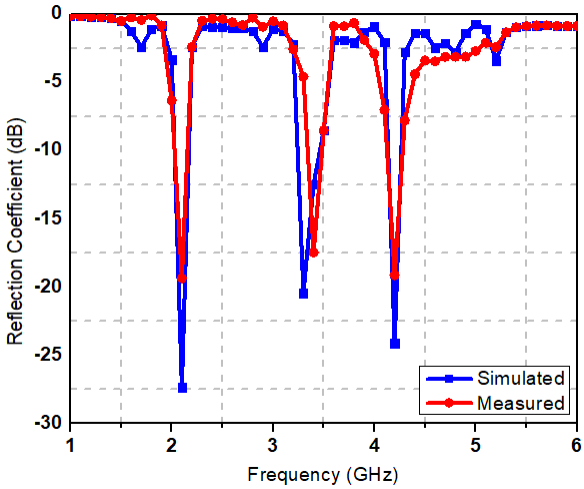

Fig. 5. Simulated versus measured reflection coefficient of the SRRRPA.

With these viable performances, it claims its efficient application in the three chosen bands of frequencies. Table 2 summarizes the results, which show the matching between the simulated and experimental results. In this section, a comparison of the converged design is presented with a couple of other research work on sub-6 GHz of frequency, summarized in Table 3. where λ_{mid} is the wavelength at the middle of the frequency, i.e., between the highest and the lowest frequency of operation in the multi-band operation.

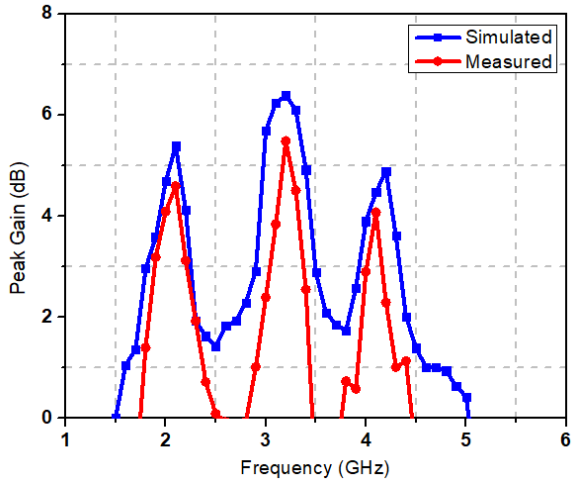

Fig. 6. Simulated and measured gain of the SRRRPA.

Table 2: Comparison between simulated and measured results

Freq.	Parameter	Simulated	Measured
2.1 GHz	Reflection coefficient	-27.5 dB	-19.7 dB
	VSWR	1.1	1.09
	Gain	4.5 dB	4.5 dB
	Bandwidth	200 MHz	230 MHz
3.3 GHz	Reflection coefficient	-20.5 dB	-17.5 dB
	VSWR	1.28	1.21
	Gain	6.4 dB	5.5 dB
	Bandwidth	170 MHz	190 MHz
4.1 GHz	Reflection coefficient	-24.1dB	-19.6 dB
	VSWR	1.2	1.18
	Gain	4.3 dB	4.1 dB
	Bandwidth	200 MHz	220 MHz

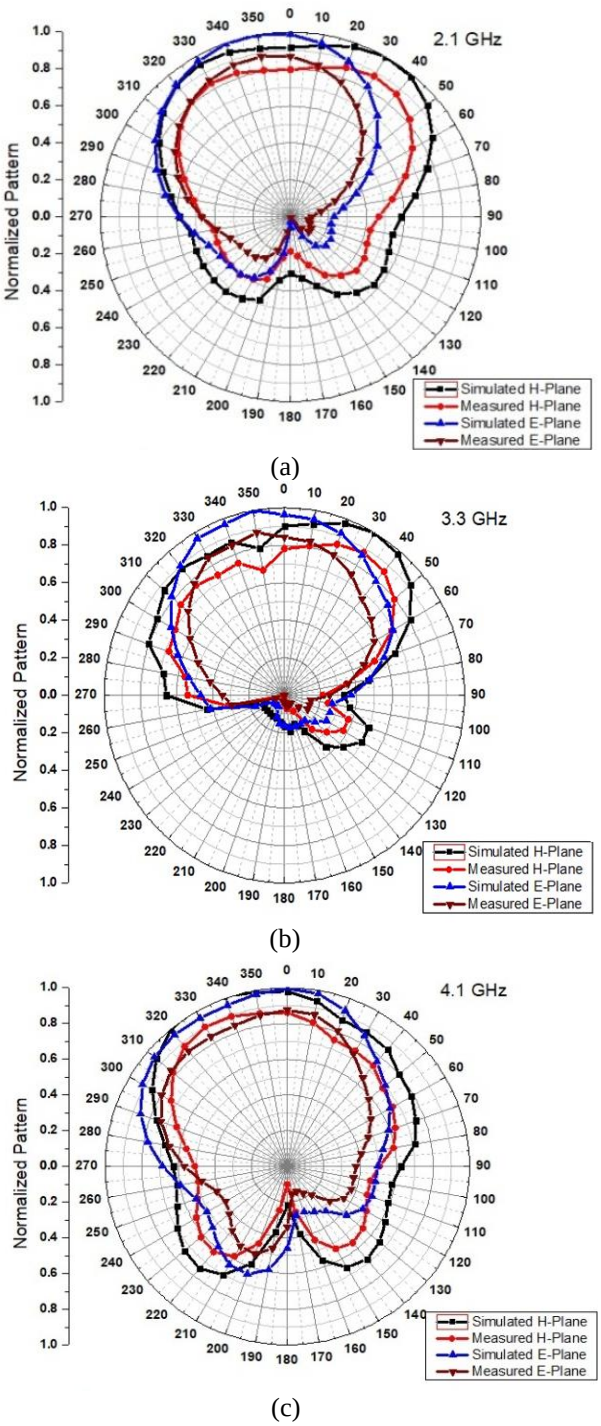

Fig. 7. Normalized radiation patterns of the SRRRPA: (a) 2.1 GHz, (b) 3.3 GHz, and (c) 4.1 GHz.

IV. CONCLUSION

In this manuscript, the design of the multi-band antenna, to be operated in sub-6 GHz 5G spectrum, is presented consisting of three bands of operating frequency. The compact microstrip antenna loaded with an inverted-F slotted fractal stub matching structure is suitable for applications in LTE-A and 5G-NR mobile technology. In the design process, investigation on fractal slots and inverted- F slot on the antenna patch is analyzed to demonstrate multi-band behavior with a higher order of precision. The symmetrical fractal lies at the edge of the length, whereas inverted-F slots are opposite to each other. The exact frequency resonance is controlled by these specified structures. A stub-matched technique along with SRR slot in the feeding is used to improve the impedance matching. The three resonating bands are precisely at 2.1 GHz, 3.3 GHz, and 4.1 GHz. The proposed antenna configuration shows a good gain response up to 6.4 dB. The antenna exhibits good impedance bandwidth up to 400 MHz and also shows the enhanced gain of more than 5 dB at all three bands. The proposed antenna is suitable for future mobile communication systems to cover up the integration of 5G with the existing LTE technology. The precise resonating frequency is highly recommended for the upcoming industry application of 5G technology.

Table 3: Comparison of the proposed SRRRPA with the state of art literature

Ref.	Resonant Frequencies (GHz)	Substrate Material	Bandwidth (GHz)	Peak Gain	Size
[3]	3.5, 5.5	FR4 with ε_r=4.4	3.400-3.800, 5.150-5.925	13 dB	$2.30\lambda_{mid} \times 1.22\lambda_{mid} \times 0.01\lambda_{mid}$
[5]	2.4, 5.2, 5.8, 26	Rogers RT5880 with ε_r = 2.2	2.450-2.495, 5.0-6.3, 23-28	4.72 dB at 5.8 GHz	$1.52\lambda_{mid} \times 1.52\lambda_{mid} \times 0.02\lambda_{mid}$
[8]	1.57, 2.45, 3.5, 5.2	FR4 with ε_r=3.5	1.575-1.665, 2.4-2.545, 3.27-3.97, 5.17-5.93	5.02 dB at 3.5 GHz	$0.6\lambda_{mid} \times 0.2\lambda_{mid} \times 0.01\lambda_{mid}$
[9]	3.3, 3.8	FR4 with ε_r=4.4	3.3-4.2, 3.3-3.8	2.5 dB at 3.5 GHz	$0.42\lambda_{mid} \times 0.18\lambda_{mid} \times 0.01\lambda_{mid}$
[10]	6, 10, 15	FR4 with ε_r=4.4	5-7, 9-10.8, 14-15	5.85 dB at 15 GHz	$0.61\lambda_{mid} \times 0.4\lambda_{mid} \times 0.1\lambda_{mid}$
[27]	0.9, 1.8, 2.4	FR4 with ε_r=4.4	0.88-0.91, 1.79-1.83, 2.39-2.42	2.12 dB at 1.8 GHz	$0.23\lambda_{mid} \times 0.08\lambda_{mid} \times 0.0.008\lambda_{mid}$
[28]	2.45, 3.5, 4.65	FR4 with ε_r=4.4	2.42-2.48, 3.3-3.7, 4.45-4.85	3.68 dB at 4.65 GHz	$0.38\lambda_{mid} \times 0.55\lambda_{mid} \times 0.01\lambda_{mid}$
[29]	1.422, 1.791, 2.467	FR4 with ε_r=4.4	1.409-1.437, 1.723-1.911, 1.858-2.045	3.276 dB at 1.422 GHz	$0.21\lambda_{mid} \times 0.16\lambda_{mid} \times 0.009\lambda_{mid}$
[30]	2.43, 3.3, 6.1	FR4 with ε_r=4.4	2.39-2.48, 3-3.7, 5-7	5 dB at 3.5 GHz	$0.40\lambda_{mid} \times 0.50\lambda_{mid} \times 0.02\lambda_{mid}$
Proposed antenna	2.1, 3.3, 4.1	Rogers RT5880 ε_r = 2.2	2-2.4, 3.3-3.6, 4-4.4	6.4 dB at 3.3 GHz	$0.46\lambda_{mid} \times 0.46\lambda_{mid} \times 0.01\lambda_{mid}$

REFERENCES

[1] R. Kumari and M. Kumar, "Design of multiband antennas for wireless communication," *International Conference on Communication Systems and Network Technologies*, Gwalior, pp. 1-6, 2013.

[2] M. Ko, H. Lee, and J. Choi, "Planar LTE/sub-6 GHz 5G MIMO antenna integrated with mmWave 5G beamforming phased array antennas for V2X applications," *IET Microwaves, Antennas & Propagation*, vol. 14, no. 11, pp. 1283-1295, 2020.

[3] Y. Li, C. Sim, Y. Luo, and G. Yang, "Multiband 10-antenna array for sub-6 GHz MIMO applications in 5G smartphones," *IEEE Access*, vol. 6, pp. 28041-28053, 2018.

[4] A. Kapoor, R. Mishra, and P. Kumar, "Analysis and design of passive spatial filter for sub-6 GHz 5G communication systems," *Journal of Computational Electronics*, 2021.

[5] Z. Khan, M. H. Memon, S. U. Rahman, M. Sajjad, F. Lin, and L. Sun, "A single-fed multiband antenna for WLAN and 5G applications," *Sensors*, vol. 20, no. 21, pp. 6332, Nov. 2020.

[6] J. Bao, Q. Huang, X. Wang, and X. Shi, "Compact multiband slot antenna for WLAN/WiMAX operations," *International Journal of Antennas and Propagation*, vol. 2014, 7 pages, 2014.

[7] B. Maity and S. K. Nayak, "Compact CPW-fed multiband F-shaped slot antenna for wireless communications," *International Conference on Wireless Communications Signal Processing and*

Networking (WiSPNET), Chennai, India, pp. 92-96, 2020.

[8] Y. F. Cao, S. W. Cheung, and T. I. Yuk, "A multiband slot antenna for GPS/WiMAX/WLAN systems," *in IEEE Transactions on Antennas and Propagation*, vol. 63, no. 3, pp. 952-958, 2015.

[9] A. Kapoor, R. Mishra, and P. Kumar, "Compact wideband printed antenna for sub-6-GHz fifth-generation applications," *International Journal on Smart Sensing and Intelligent Systems*, vol. 13, no. 1, pp. 1-10, 2020.

[10] T. O. Olawoye and P. Kumar, "A high gain microstrip patch antenna with slotted ground plane for sub-6 GHz 5G Communications," *International Conference on Artificial Intelligence, Big Data, Computing and Data Communication Systems*, pp. 1-6, South Africa, 2020.

[11] A. Kapoor, R. Mishra, and P. Kumar, "A compact high gain printed antenna with frequency selective surface for 5G wideband applications," *Advanced Electromagnetics*, 2021, (In press).

[12] P. Yang, "Reconfigurable 3-D slot antenna design for 4G and sub-6G smart phones with metallic casing," *Electronics*, vol. 9, no. 2, p. 216, Jan. 2020.

[13] R. Addaci, F. Ferrero, D. Seetharamdoo, T. Le Huy, R. Staraj, and M. Berbineau, "Multiband multi-antenna system with new approach of PIFA bandwidth enhancement," *The 8th European Conference on Antennas and Propagation (EuCAP 2014*, pp. 2880-2883, 2014.

[14] M. Gallo, O. Losito, V. Dimiccoli, D. Barletta, and M. Bozzetti, "Design of an inverted F antenna by using a transmission line model," *Proceedings of the 5th European Conference on Antennas and Propagation (EUCAP)*, Rome, pp. 635-638, 2011.

[15] R. G. Villanueva, R. L. Miranda, J. A. Tirado-Mendez, and H. Jardon Aguilar, "Ultra-wideband planar inverted-F antenna (PIFA) for mobile phone frequencies and ultra-wideband applications," *Progress In Electromagnetics Research C*, vol. 43, pp. 109-120, 2013.

[16] M. Mabaso and P. Kumar, "A dual band patch antenna for bluetooth and wireless local area network applications," *International Journal of Microwave and Optical Technology*, vol. 13, no. 5, pp. 393-400, 2018.

[17] K. Yu, Y. Li, and W. Yu, "A compact triple band antenna for bluetooth, WLAN and WiMAX applications," *Applied Computational Electromagnetics Society Journal*, vol. 32, no. 5, pp. 424-429, 2017.

[18] M. Mabaso and P. Kumar, "A microstrip patch antenna with defected ground structure for triple band wireless communications," *Journal of Communications*, vol. 14, no. 8, pp. 684-688, 2019.

[19] V. G. Raviteja, V. R. Lakshmi, and S. N. Reddy, "Multiband planar inverted-F antenna employing rectangular SRR for UMTS and WiMax/WiFi applications," *International Journal of Computer Applications*, vol. 182, no. 36, pp. 36-39, 2019.

[20] IMT Vision – Framework and overall objectives of the future development of IMT for 2020 and beyond, ITU, https://www.itu.int/dms_pubrec/itu-r/rec/m/R-REC-M.2083-0-201509-I!!PDF-E.pdf, Feb. 2014, Accessed on June 27, 2021.

[21] White paper on Enabling 5G in India, https://www.trai.gov.in/sites/default/files/White_Paper_22022019.pdf. Feb. 2019, Accessed on June 27, 2021.

[22] R. Garg, *Microstrip Antenna Design Handbook*. Artech house, Inc., 2001.

[23] A. Azari, "A new ultra wideband fractal monopole antenna," *Applied Computational Electromagnetics Society Journal*, vol. 26, no. 4, pp. 348-352, 2011.

[24] D. M. Nashaat, H. A. Elsadek, and H. Ghali, "Single feed compact quad-band PIFA antenna for wireless communication applications," *IEEE Transactions on Antennas and Propagation*, vol. 53, no. 8, pp. 2631-2635, 2005.

[25] M. Singh, V. Marwaha, A. Thakur, H. S. Saini, and N. Kumar, "Design of a low return loss planar inverted F antenna (PIFA) for 4G & WLAN," *3rd International Conference on Signal Processing and Integrated Networks (SPIN)*, pp. 539-543, 2016.

[26] Z. Lin and H. Tun, "Design and fabrication of a planar inverted-F antenna (PIFA) for LEO satellite application," *American Journal of Electromagnetics and Applications*, vol. 8, no. 1, pp. 28-32, 2020.

[27] X. Sun, "Design of a triple-band antenna based on its current distribution," *Progress In Electromagnetics Research Letters*, vol. 90, pp. 113-119, 2020.

[28] Pragati, S. L. Tripathi, S. R. Patre, S. Singh, and S. P. Singh, "Triple-band microstrip patch antenna with improved gain," *International Conference on Emerging Trends in Electrical, Electronics and Sustainable Energy Systems (ICETEESES–16)*, pp. 106-110, 2016.

[29] R. K. Verma and D. K. Srivastava, "Design and analysis of triple band rectangular microstrip antenna loaded with notches and slots for wireless applications," *Wireless Personal Communications*, pp. 1-18, 2020.

[30] D. L. Jin, T. T. Bu, J. S. Hong, J. F. Wang, and H. Xiong, "A tri-band antenna for wireless applications using slot-type SRR," *Applied Computational Electromagnetics Society Journal*, vol. 29, no. 1, pp. 47-53, 2014.

Ranjan Mishra is working as an Associate Professor in the Department of Electrical and Electronics Engineering, UPES, Dehradun, India. He received his Ph.D. in Microstrip Antenna Design from University of Petroleum and Energy Studies, Dehradun in the year 2016. He is the author of 20 Scopus indexed refereed journal and international conference papers and 4 edited books.

Rajeev Dandotiya is an engineering graduate in Electronics. He has received Ph.D. from UPES Dehradun. He has a 13 years of experience in Research and Development in the area of sensor, wireless communication, antenna design, cyber platform, and developing communication systems for industry.

Ankush Kapoor is currently pursuing his Ph.D. degree from UPES Dehradun. He has around 8 years of experience in academics. Currently, he is appointed as an Assistant Professor in Department of ECE, JNGEC Sundernagar, India. His research interests include frequency selective surfaces, design and analysis of microstrip antennas and metamaterials.

Pradeep Kumar received his Bachelor's degree, M.Eng. and Ph.D. in Electronics and Communication Engineering in 2003, 2005 and 2009, respectively. He completed his postdoctoral studies from Autonoma University of Madrid, Spain. At present, he is working with University of KwaZulu-Natal, South Africa. His current research areas include design and analysis of microstrip antennas, antenna arrays, wireless communications etc.